

EFFECT OF MECHANICAL STRESS ON THE MODES OF CORROSION OF ZIRCONIUM ALLOYS. THEORETICAL APPROACH.

V.V. Likhanskii*, T.N. Aliev, I.A. Evdokimov, M.Yu.Kolesnik, V.G. Zborovskii
SRC RF TRINITI, 142190, Troitsk, Moscow Reg., Russia
E-mail of corresponding author: likhansk@mail.ru

ABSTRACT

The paper deals with two theoretical problems in Zr-alloys corrosion. The first task is aimed to predict effect of variation in alloy composition on susceptibility of the alloy to nodular corrosion. The effect may be due to a feedback between the concentration of alloying atoms in the oxide film and the rate of oxygen transfer through the oxide film. Redistribution of alloying elements near the oxide-metal interface during the development of nodules may occur as a result of the drift of alloying additives in the field of mechanical stress. The second task is directed to determine parametric dependences for transition in oxidation kinetics. The transition in oxide growth kinetics may depend on the properties of zirconium alloy and oxide film. Parametric criterion for the transition was derived in the framework of theoretical analysis. The analysis assumed minimization of mechanical energy in the system 'oxide film – metal' with taking into account possible formation of periodic structures at the oxide-metal interface.

INTRODUCTION

Corrosion behavior of zirconium alloys depends on several factors, such as chemical composition of the alloy, its microstructure, and operating conditions. Microstructure of the alloy depends on both chemical composition and technology of production. Operating conditions are determined by coolant temperature and pressure, water chemistry, heat flux and characteristics of neutron field.

For justification operating conditions and lifetime of fuel assembly, mainly engineering models of zirconium corrosion are used. Several models were developed for different zirconium alloys, [1,2]. Most of these engineering models are based on correlations and are designated to predict oxidation kinetics and hydrogen content in the alloy.

Additional work should be performed to validate corrosion behavior of zirconium alloys when fuel operating conditions are changed (neutron field, water chemistry, operation lifetime) and/or when alloy chemical composition and microstructure are varied to provide better alloy performance. The investigation is necessary to meet the existing criteria of alloy oxidation under the changed conditions. Application of correlation models beyond the experimental conditions under which they were derived, often leads to significant errors. More effective approach is based on using physical models and getting parametric dependences on the basis of them.

ADDITIVES EFFECT ON ZIRCONIUM ALLOYS SUSCEPTIBILITY TO NODULAR CORROSION

At present time, there are few phenomenological models considering different physical mechanisms of nodular corrosion [3-5]. This work advances theoretical approach [6], where the effect of small changes in alloying additives concentrations on the evolution of initial stage of nodule formation is investigated. Growing nodule is considered as small perturbation of oxide-metal boundary. If addition of additive atoms may decrease initial perturbation at time lower, than experimentally observed time of nodule formation, such an alloying may be considered as effective means for suppression of nodular corrosion. Perturbation of flat corrosion front evokes heterogeneous mechanical stresses as a result of difference in zirconium and zirconium oxide density. Drift of alloying elements in this mechanical stress leads to the redistribution of alloying atoms at perturbed corrosion front. Alloying additives, depending on its valence, influence on oxygen vacancy concentration and on tetragonal phase fraction. This brings change in oxygen transport rate and, as a consequence, changes in local oxidation rate. As a result, initial perturbation may growth or depress. The magnitude of mechanical stress, that provoke drift of alloying elements, was evaluated on dimensional grounds. The point of this work has additions to theoretical analysis of [6]. At first, analytical solutions for mechanical stresses in oxide and metal are included. This allows to take into account an initial perturbation wavelength, oxide thickness, mechanical properties of zirconium and zirconium oxide. Second, the case, when equilibrium distribution of alloying element establishes in mechanical stresses field due to fast diffusion, is considered. Third, some effects, concerned with the presence of precipitates in Zr-alloys are considered. Obtained results are applied for the analysis of susceptibility of Zircaloy-2,-4 modifications to nodular corrosion.

Mechanical Stress Field Due to Perturbation of the Metal-Oxide Interface. Let's consider a periodic perturbation of the oxidation front $\tilde{l} \sin(\chi_{\perp} x)$. Characteristic scale of the perturbation $\sim \pi \chi_{\perp}^{-1}$ may be governed by a size of nodule nuclei ($\sim 1 \mu\text{m}$) or by a distance between neighboring precipitates ($\sim 0.2-1 \mu\text{m}$). Below we assume that the oxide thickness $2h$ is much less than thickness of the metal layer and consider perturbations with small amplitude, $\tilde{l} \ll 2h, 2\pi/\chi_{\perp}$. For thin oxide films, $2h\chi_{\perp} < 1$, it may be supposed that perturbation of the oxide-metal interface is equivalent to periodic homogeneous variation of the oxide volume. In mathematical terms, the corresponding mechanics problem is reduced to double-layer system with periodic perturbation of specific volume in one of the layers.

$$\delta = (\varepsilon - 1) \frac{\tilde{l}}{2h} \sin(\chi_{\perp} x) = \delta_0 \sin(\chi_{\perp} x). \quad (1)$$

Here $\varepsilon = 1.56$ is the ratio of Zr to ZrO_2 density (the Pilling-Bedworth ratio).

Plain strain is assumed so that displacements along z -axis are all zero. Solution of this problem is expressed in terms of elastic stress potential φ in the oxide and in the metal, [7]:

$$\sigma_{xx} = \frac{\partial^2 \varphi}{\partial y^2}, \quad \sigma_{yy} = \frac{\partial^2 \varphi}{\partial x^2}, \quad \tau_{xy} = -\frac{\partial^2 \varphi}{\partial x \partial y}. \quad (2)$$

The elastic potential in the oxide layer and in the metal is found from the inhomogeneous equations

$$\Delta \Delta \varphi^{ox} = -\frac{E_{ox} \Delta \delta}{3(1-\nu_{ox})}, \quad \Delta \Delta \varphi^{me} = 0 \quad (3)$$

where E_{ox} is the Young modulus and ν is the Poisson ratio for the oxide. In the metal the equation has a form.

Boundary conditions correspond to continuity of normal and tangential stress at the oxide boundaries as well as to continuity of normal and tangential displacements at the metal-oxide interface. For arbitrary wavelengths the problem was solved numerically. The analytic asymptotics were obtained for $2h\chi_{\perp} \ll 1$.

Mechanical stress derived for the undulated oxide-metal interface may be applied to analyze the effect of alloying additives on resistance of the alloy to nodular corrosion. For long-wave undulations ($\chi_{\perp} \ll u_0/D_{ad}$) of small amplitude, ($|\tilde{l}^{-1} \partial \tilde{l} / \partial t| \ll u_0^2 / 4D_{ad}$), perturbation of the corrosion front evolves in time according to the following simplified expression:

$$\frac{\partial \tilde{l}}{\partial t} \sim -\frac{\tilde{l}}{u_0} \left(\frac{\partial u_0}{\partial C_m} \right) C_m (1-\alpha) \cdot D_{ad} \chi_{\perp}^2 \cdot \left(-1 + \frac{A_{im}}{\kappa_b T} \right). \quad (4)$$

Here u_0 is the propagation velocity of the corrosion front, C_m is the solute concentration of the additive in the metal, α is the ratio between additive solubilities in Zr and ZrO_2 , D_{ad} is the additive diffusivity in the metal, κ_b is the Boltzmann constant, T is the temperature. Stress-induced drift of alloying atoms is described by the factor of

$$\frac{A_{im}}{\kappa_b T} = -\frac{\Phi_0}{\tilde{l} \chi_{\perp} \kappa_b T} \equiv F(h\chi_{\perp}) \frac{\Omega}{V_{Zr}}, \quad (5)$$

where V_{Zr} is the volume of zirconium atom in α -Zr lattice, Ω is the dilatation volume for alloying atom, $F(h\chi_{\perp})$ is the dimensionless function of wavelength, oxide thickness and the elastic constants of the oxide and the metal (E_{ox} , ν). The function F is inversely proportional to temperature. Φ_0 in Eq.(5) is the amplitude of free energy in the metal in the vicinity of the metal-oxide boundary, [8]:

$$\Phi_0 \sin(\chi_{\perp} x) = -\Omega \text{sp}(\sigma) \Big|_{y=h} / 3. \quad (6)$$

In the case of plane strain, $sp(\sigma) \equiv \sigma_{xx} + \sigma_{yy} + \sigma_{zz} = (1 + \nu)(\sigma_{xx} + \sigma_{yy})$. The gradient of free energy, Eq.(6), defines the drift velocity of alloying atoms. For small perturbation amplitudes strain is elastic and $sp(\sigma) \sim \tilde{l}$. Numerical solution for $sp(\sigma)|_{y=h}$ and analytical asymptotes for it are demonstrated in Fig.1.

It follows Eqs.(4)-(5), that for a fixed wavelength the contribution of the stress-induced drift to the rate of perturbation evolution decreases as the oxide grows on. This fact could explain why nucleation of nodules occurs after some incubation period. Indeed, the characteristic wavelength of perturbations may be governed by ‘external’ parameters such as, e.g., a distance between precipitates or specified oxidation conditions. In this case variations in spatial scale of undulations would be minor during oxidation. While the oxide layer is thin ($h\chi_{\perp} \ll 1$), the drift term will play the leading role in the right-hand part of Eq.(4). If the stress-induced drift of alloying additive provides a negative feedback and stabilize perturbations, initiation of nodular oxidation will be suppressed. When the oxide layer is getting thicker so that contribution of the stress-induced drift diminishes, the right-hand part of Eq.(4) may change in sign. From this point on, the growth of nodules is possible. Incubation period before initiation of nodular oxidation is observed experimentally,[9].

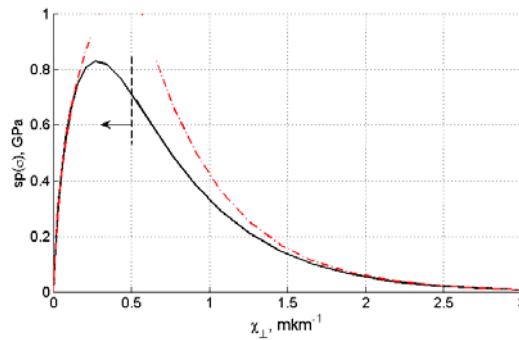


Fig.1. Amplitude of $sp(\sigma)$ in the metal in the vicinity of the oxide-metal interface as a function of χ_{\perp} . Solid line is the numerical solution, dotted lines represent the analytical asymptotes. Calculated for $2h = 2 \mu\text{m}$, $\tilde{l}/2h = 0.1$. The range of the model validity $2h\chi_{\perp} < 1$ is marked with arrow.

Consider a diffusive transfer of alloying element (disregarding its drift in the field of mechanical stress) when undulation evolves at the oxide-metal interface. If we take a plane in the metal parallel to the plane of the undisturbed corrosion front, solute concentration of additive will be different in areas where undulation penetrates ahead or falls behind the front of uniform oxidation (see Fig.2 for illustration).

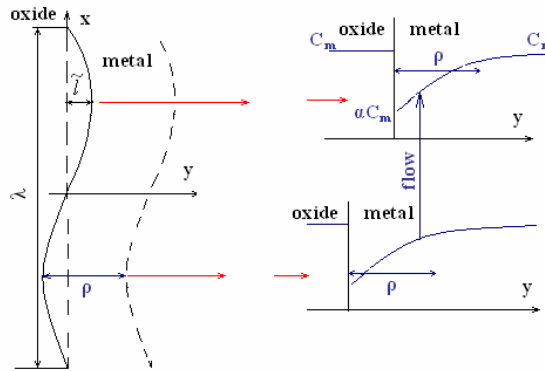


Fig.2. Concentration profile of solute iron in the metal near the corrosion front.

The perturbation evolves according to the following rule

$$d\tilde{l}/dt \sim \Delta\tilde{C}(\partial u_0/\partial C). \tag{7}$$

Here, $\Delta\tilde{C}$ is the change in local solute concentration of additive in the metal in areas. Variations in additive concentration along the oxidation front tend to flatten out due to diffusion. If an additive has higher solubility in the oxide than in the metal, its concentration is lower near the oxide-metal interface (Fig.2). Such alloying additives will diffuse to areas of accelerated corrosion. On the contrary, additives with lower solubility in the oxide will diffuse to areas with slower oxidation. Characteristic time of diffusive transfer is

$$\Delta\tau \sim \rho/u_0, \quad (8)$$

where ρ is the spatial scale of the diffusion profile near the oxide boundary, Fig.2. In a time period, defined by Eq.(6), the change in concentration will be $\Delta\tilde{C} \sim \frac{\tilde{l}}{u_0} D_{ad} \chi_{\perp}^2 C_m (1-\alpha)$ and the following expression is similar to (4):

$$\frac{d\tilde{l}}{dt} \sim \frac{\tilde{l}}{u_0} \left(\frac{\partial u_0}{\partial C} \right) C_m (1-\alpha) D_{ad} \chi_{\perp}^2. \quad (9)$$

Transfer of the additive due to the stress-induced drift may be taken into account in a similar way. Direction of the drift, as mentioned above, is governed by relation of atomic sizes.

The derived expressions evidence that the decrement value does not depend on diffusion scale ρ . This occurs because higher concentration gradient leads to lower characteristic transport time $\Delta\tau$. In absence of precipitates, the scale ρ is equal to D_{ad}/u_0 . Precipitates may lead to more sharp profile of the solute concentration in the metal in close vicinity to the corrosion front. It may happen if the alloying element is quickly redistributed into Zr-matrix when precipitates come into the area of reduced solute concentration. But, as shown, this effect wouldn't influence the decrement value, Eq.(4).

Theoretical approach [6] is applicable for perturbations with wavelength in excess of $\lambda > \lambda_{cr}$, where λ_{cr} is the characteristic migration length for time $\Delta\tau$:

$$\lambda_{cr} \approx \sqrt{D_{ad} \Delta\tau} = D_{ad}/u_0. \quad (10)$$

In the opposite limiting case $\lambda \ll \lambda_{cr}$ which is relevant to fast diffusion of solute additive, the resulting equilibrium concentration of alloying elements in the metal for harmonic undulations is defined as:

$$C(x)|_{\text{interface}} = \alpha C_m \exp\left(-\frac{\Phi_0 \sin(\chi_{\perp} x)}{\kappa_b T}\right). \quad (11)$$

The corresponding local variation in the corrosion rate is described by equation

$$\frac{\partial \tilde{l}}{\partial t} = \left(\frac{\partial u}{\partial C_m} \right) \Delta\tilde{C}|_{\text{interface}} = \left(\frac{\partial u_0}{\partial C} \right) \alpha C_m \frac{\Omega \text{sp}(\sigma)}{3\kappa_b T} = \tilde{l} \chi_{\perp} \left(\frac{\partial u_0}{\partial C} \right) \alpha C_m F(h\chi_{\perp}) \frac{\Omega}{V_{Zr}}. \quad (12)$$

DISCUSSION

The results of the analysis are applied to additives of Fe, Cr, Ni and Sn in Zircaloy-2 and Zircaloy-4. Atomic radii of Fe, Cr and Ni in α -Zr are close to each other. According to ab-initio calculations in [9], difference in energies for Ni atom in interstitial and substitution sites in α -Zr is about 0.86 eV. It means that a preferred position for nickel atom in α -Zr is a substitution site. It may be supposed, that Fe and Cr atoms also occupy preferably the substitution positions. As far as atomic radii of Fe, Cr and Ni are lower than that of Zr, [10], the derivative $\partial u_0/\partial C_{ox}$ in Eq.(4) is positive, since addition of Fe, Cr and Ni tends to accelerate uniform corrosion, [4]. This effect is a consequence of increased concentration of oxygen vacancies in the oxide.

Effect of Iron and Nickel. The characteristic scale λ_{cr} for iron and nickel in Zircalloys exceeds a value of ~ 10 μm . It is much more than thickness of the pre-transition oxide film. So, to estimate the effect of Fe and Ni on evolution of long-wave perturbations ($\lambda > \lambda_{cr}$), we have to use Eq.(4) in the limit of thin oxide layer. In this case the stress-induced drift is dominating and the right-hand part of Eq.(4) is negative. For short-wave perturbations, ($\lambda < \lambda_{cr}$), we have to use Eq.(12). Its right-hand part is also negative for Fe and Ni. The final conclusion from theory is that increasing of solute concentrations of iron and nickel in the metal is a means of making the alloy more resistant to nodular corrosion. This conclusion is in agreement with experimental data. Both autoclave tests in high temperature steam and in-reactor data show that susceptibility of Zircaloy-2 and Zircaloy-4 to nodular corrosion diminishes with increase in concentration of iron and nickel in matrix, [4,11,12].

Effect of Chromium. The analysis shows that addition of chromium into Zircaloy has to be in favor of better resistance to nodular corrosion. This conclusion is confirmed by experimental results in high temperature steam,

[13,14]. However, the effect of Cr is rather moderate since its diffusivity and, hence, the decrement value, is ~ 2 orders of magnitude lower than that for iron and nickel, [10,15]. It is also in agreement with experiments [13,14]. It was reported that alloying with chromium is much less effective for enhancing resistance of Zircalloys to nodular corrosion in comparison with iron and nickel. Some effects of tin and precipitates are also considered.

PARAMETRIC CRITERION FOR “TRANSITION” IN OXIDATION KINETICS OF ZR ALLOYS

An initial growth of the oxide film mainly obeys a cubic or parabolic law till the thickness reaches about 1.5-3 μm , [1,2]. This stage of Zr alloy oxidation is called pre-transition regime of oxide film growth. However, with further film growth, the mechanical strains are increased at the metal/oxide interface, and, under certain thickness of the film, cracks are formed. Kinetics of the oxide film growth becomes quasi-linear when the oxide thickness is more than 1.5-3 μm . This oxidation stage is called post-transition and is characterized by a presence of a large number of defects in the oxide film such as cracks and pores, [16, 17]. The cracks are developing along the interface, [18,19]. Cracking provides fast access for the oxidizer to the metal-oxide interface resulting in acceleration of oxide growth.

It is proposed [18, 19], that the oxide film growth during quasi-linear stage is determined by transition parameters. Occurrence of the transition in oxidation kinetics of zirconium alloys is due to the stress growth close to the oxide/metal interface, [20-23]. Mechanical stresses are increased with the thickness of the oxide film because of significant difference in specific volume of oxide and metal. Formation of wavy structures was often observed at the oxide film-metal interface, [22,23]. In some publications it has been suggested that development of such wavy structures precedes the transition in kinetics of the oxide film growth. Absence of reliable theoretical models makes experiments the only way to find optimal materials.

According to experiments [18, 19], a transition in oxidation kinetics occurs as a result of cracks formation in oxide film. We have also assumed that a wavy structure in vicinity of the metal/oxide interface was formed before cracking in the protective oxide layer. Let's calculate mechanical energy of deformations in the metal-oxide system to find conditions for the oxide film cracking. We have determined the thickness of the oxide film which makes formation of a wavy structure “energy-profitable” and may lead to oxide cracking. Such conditions may correspond to occurrence of a transition in oxidation kinetics.

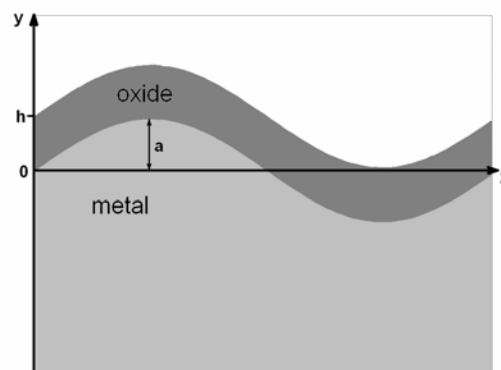


Fig.3. Scheme of oxide/metal wavy structure.

The volume expansion during a transition from the metal to the oxide is anisotropic [18, 19]. The volume growth of the oxide is carried out significantly by expanding in the direction of free surface. But even small increase of the lattice size in the plane of an oxide leads to essential stresses. This anisotropy appears due to the oxide microstructure. Columnar grains of monoclinic phase (m-phase) are elongated in the direction perpendicular to the interface. Grains of tetragonal phase (t-phase), stabilized by compressive stresses in the film, can be located between the monoclinic columnar grains. This microstructure leads to mechanical anisotropy of the oxide.

Let's assume that the interface between an oxide film and a metal is planar and the thickness of the oxide is uniform at the initial oxidation stage. The mechanical energy increases both in the oxide and in the metal with increasing of the oxide film thickness. The planar oxide film could have energy benefit from creation of a wavy structure of the oxide, Fig.3. The transition to a wavy structure leads to expansion of the oxide surface and in this way decrease the compressive energy of the oxide film. However, there is the energy associated with the bending deformation of the oxide film and the metal mechanical energy which is localized in vicinity of the interface. Following calculations are carried out for deformation energy change with a wavy structure formation according with geometry of Fig.3.

Suppose a wavelength of a periodic structure is $\lambda=2\pi/k$ (k – wave vector), a is a wave amplitude, h is thickness of an oxide film, ε is a coefficient of linear expansion in the plane of interface during a transition

from the metal to the oxide. A mechanical energy change per unit area in a system metal/oxide film $\Delta U_{m,ox}$ for small amplitude of a forming periodic structure $ka \ll 1$ is:

$$\Delta U_{m,ox} = -\frac{(ka)^2}{8\varepsilon} \frac{hE_{ox}}{(1-\nu^2)} \left(\frac{2(\varepsilon-1)}{\varepsilon} - \frac{(ka)^2}{4\varepsilon} \right) + \frac{E_{ox}(kh)^3 ka^2}{48(1-\nu^2)} \beta + \frac{E_m ka^2}{8(1-\nu_m^2)} \quad (13)$$

The first term is the change in the compressive energy of the oxide film, the second is bending energy of a unit area of the oxide film and the third is mechanical energy per unit area in the metal. Here E_{ox} is the Young modulus of the oxide, ν – Poisson ratio of the oxide, E_m is Young modulus in the metal, ν_m is Poisson ratio in the metal. Eq.(13) is valid in the frame of elasticity theory.

The β coefficient is used to take into consideration anisotropic mechanical properties of the oxide film and its plasticity under bending deformations. As a rule, oxide film in the vicinity of interface consists of columnar grains of monoclinic phase which is oriented perpendicular to the interface, and grains of tetragonal phase [20]. Alloying elements, which are poorly soluble in the oxide, may be located between the columnar grains. Therefore the bending energy is lower compared to an isotropic single-crystal oxide, $\beta < 1$. Absence of expressed smoothing of the wavy boundary oxide/metal after dissolution of metal under oxide with the acid ([24,25]) evidences in favor the β parameter to be significantly less than 1.

If the wave amplitude exceeds the yield stress, $\sigma_{cr} \approx \sigma_{0.2}$, the total energy change in metal deformation will involve elastic and plastic part:

$$\Delta U_{m,ox} = -\frac{(ka)^2}{8\varepsilon} \frac{hE_{ox}}{(1-\nu^2)} \left(\frac{2(\varepsilon-1)}{\varepsilon} - \frac{(ka)^2}{4\varepsilon} \right) + \frac{E_{ox}(kh)^3 ka^2}{48(1-\nu^2)} \beta + \frac{1}{2} \sigma_{cr} \left(a - \sigma_{cr} \frac{(1-\nu_m^2)}{kE_m} \right). \quad (14)$$

Here $\sigma > \sigma_{cr}$ and $a \geq 2\sigma_{cr} (1-\nu_m^2) / kE_m$.

The transition criterion in oxidation kinetics includes realization of two conditions. First, a wavy structure formation should be energetically “profitable”. Second, the wave amplitude should exceed a critical value. The local stresses for the wavy amplitude should be higher than a breaking point for metal/oxide boundary or the yield limit will be exceeded. Note, the highest tensile stresses in the metal are realized in regions of the “wave” behind the front of corrosion. So, appearance of structural defects such as cracking should be expected in such regions. A wavy structure formation at the metal/oxide interface starts at a critical value of oxide thickness, h_{cr} . Conditions of wavy structure formation can be defined from the provided inequality:

$$d\Delta U_{m,ox}(k, h > h_{cr}) / da^2 < 0, \text{ at } a = 0.$$

Let's evaluate typical values for the parameters in (13,14). Young's modulus ratio is in the range $E_{ox}/E_m = (2 \div 3)$ [22, 26], linear expansion coefficient of phase transition from the metal to its oxide in the plane of the interface is slightly more than 1, $(\varepsilon-1) \ll 1$. The value of $(\varepsilon-1)$ was measured experimentally from the dependence of deviation of a zirconium plane end versus thickness of the oxide layer in sided oxidation, [19, 27]. However, in those experiments, as it has been discussed in [19], value of $(\varepsilon-1)$ was calculated without taking into account two factors: wavy structure, which was observed in the experiments, and plastic deformations in metal in vicinity of the interface. If those two factors, which reduce the value of $(\varepsilon-1)$ parameter, are not taken into account, the efficient value of the parameter, estimated from experimental data, is less than 0.5%, [27]. Not the effective parameter $(\varepsilon-1)$, but real value of linear elongation coefficient due to oxide formation have considered in the theoretical approach. Therefore, we have used value $(\varepsilon-1) \sim (1 \div 5) \cdot 10^{-2}$ for estimates, which is more than one measured in experiments. Note, formation of undulating structure with the amplitude to period ratio $\sim 7 \cdot 10^{-2}$, which is less than the value measured in experiments [19, 27], is enough to compensate for the linear increase of about $5 \cdot 10^{-2}$ even without taking into account stresses occurrence. Analysis of the equation (13) gives conditions for “spontaneous” formation of a wavy structure at the oxide/metal boundary:

$$\beta < \frac{64}{9} (\varepsilon-1)^3 \left(\frac{E_{ox}}{E_m} \right)^2 \quad (15)$$

If the next parameters are chosen: $E_{ox}/E_m = 3$ and $(\varepsilon - 1) = 5 \cdot 10^{-2}$, the value of β should be less than $8 \cdot 10^{-3}$ for a formation of periodic structure. For $\beta = 5 \cdot 10^{-3}$ the structure wavelength λ could be found in the range $(0.57 \div 1.9)h$. For deformations, when a plastic changes in the metal can be neglected, a wavy structure amplitude is determined from the condition of energy minimum (13):

$$ka = 2 \sqrt{(\varepsilon - 1) - \frac{\varepsilon^2}{2} \left(\frac{E_m}{khE_{ox}} + \frac{(kh)^2 \beta}{6} \right)} \quad (16)$$

The amplitude corresponding to the minimum of the mechanical energy in the system in the assumption of elastic deformations in metal is realized at $(kh) = (3E_m / \beta E_{ox})^{1/3}$. A reduction of parameter β (reduction of “cross-links” between the columnar grains of m-phase in oxide film) leads to undulation amplitude increase. For above chosen parameters E_{ox}/E_m , $(\varepsilon - 1)$ and β , the ratio $2a/\lambda$ is 5.4%. Plastic deformations in metal can be realized at such value of deformations. In this case $\sigma > \sigma_{cr}$, the wavelength of the wavy structure as far as amplitude are determined from the condition of minimum of energy, (14). Numerical analysis has showed that the plastic deformation in metal had been realized. The qualitative dependencies were the same and undulation amplitude grows with reduction of β parameter.

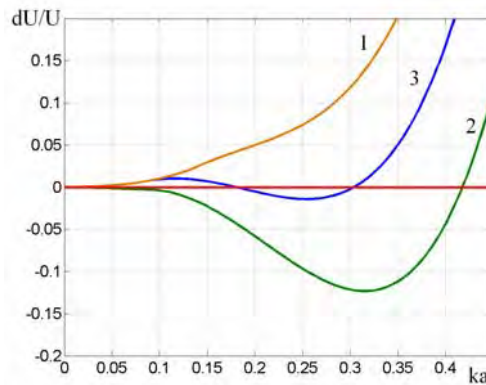


Fig.4. Energy change against wavy structure amplitude.

1 – Formation of wavy structure is “unprofitable”, 2 – plane front is unstable with respect to small perturbations, 3 – formation of a structure with amplitude high the threshold value is “profitable”.

There are three different behaviors of deformation energy change depending on amplitude of wavy structure. The maximal and minimal values of the curves depend on mechanical properties of metal, oxide and on β parameter. If β satisfies (15), undulation is energetically profitable (curve 2 in Fig.4), and its spontaneous formation is possible. If β does not satisfy (15), mechanical energy increases with the amplitude at $ka \ll 1$. Energy changes versus amplitude for such β are shown in Fig.4 (curves 1, 3). Curve 1 in Fig.4 corresponds to the metal with high yield strength. Curve 3 corresponds to the metal with relatively low yield strength. If β does not satisfy (15), spontaneous formation of undulation structure is unprofitable from the minimal stress energy approach. It should be noticed that the presence of particles of a secondary phase as well as condition of spontaneous formation of undulation (Fig.4, curve 2) can lead to irregularity in metal/oxide boundary. The secondary phase particles can be a cause of irregularity formation at the metal/oxide interface with the scale close to size of the particles. If the irregularities exceed the amplitude threshold value, their growth is possible in accordance with energy curve 3, Fig.4.

CONCLUSION

Presented theoretical approach was applied to analysis of two theoretical problems. The effect of variation in alloy composition on susceptibility of the alloy to nodular corrosion was considered. The effect may be important due to a feedback between the concentration of alloying atoms in the oxide film and the rate of oxygen transfer through the oxide film. Redistribution of alloying elements near the oxide-metal interface during the development of nodules may occur as a result of the drift of alloying additives in the field of mechanical stress. The results of the analysis for Zircaloy-2,4 are in agreement with many experimental data revealing the effect of additives of Fe, Cr, Ni and Sn on susceptibility of Zircalloys to nodular corrosion.

The analysis established that the parametrical condition of oxidation “transition” gives qualitative agreement with experimental data. The analysis evidences that “transition” is caused by evolution of mechanical stresses in oxide layer and in adjacent metal layer and is related to undulation. Experiments show that a typical period and rate of undulation development at fixed oxidation conditions depend on chemical composition and microstructure of the alloy. The theoretical approach proposed in [6] gives an opportunity to relate changes in alloying elements concentration in the metal and changes of undulation development parameters.

REFERENCES

- [1] Douglass, D.L., “The Metallurgy of Zirconium”, *Int. Atomic Energy Agency*, Vienna, 1971.
- [2] Zaimovskii, A.S., Nikulina, A.V., Reshetnikov, N.G., “Zirconium alloys in nuclear power”, *Energoatomizdat*, Moscow, 1994.
- [3] Cheng, B., Adamson, R.B., “Mechanistic studies of zircaloy nodular corrosion,” *Proc. 7th Int. Symp. Zirconium in the Nuclear Industry*, Philadelphia, *ASTM STP-939*, 1987, pp.587-416.
- [4] Rudling, P., and Wikmark, G., *J. Nucl. Mater.*, 256, 1999, pp.44-59.
- [5] Ramasubramanian, N., “Out-reactor nodular corrosion behavior of zircalloys,” *J. Nucl. Mater.*, 119, 1983, p.208-218.
- [6] Likhanskii, V.V., Evdokimov, I.A., “Effect of additives on the susceptibility of zirconium alloys to nodular corrosion,” *J. Nucl. Mater.*, 392, 2009, pp.447-452.
- [7] Timoshenko, S.P., Goodier, J.N., “Theory of elasticity,” ed.3, N.Y., 1970.
- [8] Hirth, J.P., Lothe, J., “Theory of dislocations,” ed.2, Wiley, 1982.
- [9] Garzarolli, F., Stechle, H., et al, “Progress in the knowledge of nodular corrosion,” *Proc. 7th Int. Symp. Zirconium in the Nuclear Industry*, *ASTM STP 939*, 1987, pp.417-430.
- [10] Fernandes, M.G., “Fast impurity diffusion in hcp Zr,” *doctoral thesis*, Massachusetts, 1991.
- [11] Tendler, R., Abriata, J.P., “Atomic size and fast diffusion of metallic impurities in zirconium,” *J. Nucl. Mater.*, vol.150, 1987, pp.251-258.
- [12] Kruger, R.M., Adamson, R.B., Brenner, S.S., “Effects of microchemistry and precipitate size on nodular corrosion resistance of Zircaloy-2,” *J. Nucl. Mater.*, vol.189, 1992, pp.193-200.
- [13] Weidinger, H.G., et al, “Effect of chemistry on elevated temperature nodular corrosion,” *Proc. 7th Int. Symp. Zirconium in the Nuclear Industry*, *ASTM STP 939*, 1987, pp.364-386
- [14] Inagaki, M., Akahori, K., Maki, H., “Effects of alloying elements on the nodular corrosion resistance of zircaloy,” *Trans. of the American Nuclear Society*, 47, 1984, pp.177-178.
- [15] Hood, G.M., Schultz, R.J., “Diffusion of 3D transition elements in α -Zr and zirconium alloys,” *ASTM STP 1023*, Philadelphia, 1989, pp.435-450.
- [16] Bouineau, V., et. al, "In situ measurements on the metal-oxide strain tensor in case of zirconium alloy oxidation", *15th Int. Symp. on Zirconium in the Nuclear Industry*, 2007, Sunriver, OR.
- [17] Hutchinson, B., Lehtinen, B., “A theory of the resistance of zircaloy to uniform corrosion”, *Journal of nuclear materials*, vol. 217, p. 243-249, 1994.
- [18] Preuss, M., Frankel, P., et. al., “Towards a mechanistic understanding of corrosion mechanisms in zirconium alloys,” *16th Int. Symp. on Zirconium in the Nuclear Industry*, Chengdu, 2010.
- [19] Ly, A., Ambard, A., Blat, M., “Zirconium alloys microstructure effect on their corrosion kinetics: Case of Zircaloy-4,” *16th Int. Symp on Zirconium in the Nuclear Industry*, Chengdu, 2010.
- [20] Park, J.-Y., Choi, B.-K., Yoo, S.J., Jeong, Y.H., “Corrosion and Oxide Properties of HANA Alloys”, *15th Int. Symp. on Zirconium in the Nuclear Industry Sunriver*, Oregon, USA, 2007.
- [21] Tejlund, P., et. al, "Detailed microstructure of the metal/oxide interface region in Zircaloy-2 after autoclave corrosion testing", *16th Int. Symp.on Zirconium in the Nuclear Industry*, Chengdu, 2010.
- [22] Etoh, Y., Aomi, M., Ishimoto, S., Nashioka, S., Muta, H., Uno, M., Yamanaka, S., “Mechanical properties of oxide film on Zr alloys”; *LWR Fuel*, 2010.
- [23] Evans, A.G., He, M.Y., Hutchinson, J.W., “Effect of interface undulation on the thermal fatigue on thin films and scales on metal substrates”; *Acta mater.*, Vol. 45, pp.3543-3554; 1997.
- [24] Tejlund, P.,et. al, "Detailed microstructure of the metal/oxide interface region in Zircaloy-2 after autoclave corrosion testing", *16th Int. Symp.on Zirconium in the Nuclear Industry*, Chengdu, 2010.
- [25] Hutchinson, B., Lehtinen, B., “A theory of the resistance of zircaloy to uniform corrosion”, *Journal of nuclear materials*, vol. 217, p. 243-249, 1994.
- [26] Paris, M., Foerch, R., Cailletaud, G., “Coupling between diffusion and mechanics during the oxidation of zircaloy”; *J. Phys. IV France* 9; 1999.
- [27] Bouineau, V., et. al, "In situ measurements on the metal-oxide strain tensor in case of zirconium alloy oxidation", *15th Int. Symp. on Zirconium in the Nuclear Industry*, Sunriver, OR. 2007.